Predictive position control in two-mass drive with induction motor over a wide range of speed changes

Piotr J. Serkies, Grzegorz Tarchała
Wrocław University of Technology
50-372 Wrocław, ul. Smoluchowskiego 19, e-mail: piotr.serkies@pwr.wroc.pl;
grzegorz.tarchala@pwr.wroc.pl

This paper deals with the predictive shaft position control for the two-mass induction motor drive. The controller co-operates with the Direct Torque Control – Space Vector Modulation (DTC-SVM), also in the field-weakening region. The adaptation mechanism of the torques constraints is applied to ensure that the critical torque is not exceeded. Within the framework of the research the influence of the position time constant and the speed constraint level on the dynamical properties is analysed, also in the field-weakening region.

1. Introduction

One of the main aims of modern drive systems is positioning of the industrial actuators. In order to cope with the requirements, such as precision of the control, safety, response time etc., the load machine characteristic must be taken into consideration during the control structure designing – in particular the finite stiffness of the shaft. Exclusion of the shaft characteristic can lead to the torsional vibrations, which substantially deteriorate the positioning precision. In extreme cases they can cause the drive damage and the machine immobilisation [1-7].

The PI regulators-based cascade control structure with additional feedbacks is the classical algorithm for the position control of the two-mass electrical drives [1]. The methods based on the identification of the drive parameters using the Extended Kalman Filter (EKF) and tunable PI regulators [2] or control structure H^{∞} [3] can be used in this purpose, as well. In [4, 5] a concept of the regulator based on the Force Dynamic Control (FDC) law for the Permanent Magnet Synchronous Motor (PMSM) is presented. In this paper the control loop is divided into two parts (the work contains only simulation tests). In [5] the Sliding-Mode Control (SMC) structure is discussed. Obtained results are compared with the ones acquired for the cascade FDC algorithm (which is presented in [4] as well). Also in this case only simulation studies are presented. In [6] two control structures are compared: the FDC-based position regulator without the division on the position and control loops and the cascade control structure with PI regulators and additional feedbacks. In this paper experimental tests are presented as well. Articles which describe the regulators based on the nominal reference trajectories [7] have appeared in recent times. They require application of digital filters, in order to eliminate the torsional

vibrations of the shaft. In [8, 9] the predictive control is introduced in positioning of the two-mass drives.

The described publications have not dealt with the position controller co-operation with the induction motor and the possibility of its operation in the field-weakening region. Exploitation of this region can successfully reduce the times necessary to reach the reference positions, especially for large positioning constants.

This paper deals with the co-operation of the predictive position controller with the induction motor drive with elastic coupling, controlled using the Direct Torque Control with Space Vector Modulation (DTC-SVM) [10]. Simulation test results are presented to prove the positioning improvement.

2. The induction motor drive with the field-oriented control structure

Induction motors (IM) are used more and more widely in different industrial applications. They are durable, do not require much servicing and are relatively inexpensive, however they are nonlinear objects and thus require advanced control methods. IM model can be described by the equations (in any coordinate system rotating with speed ω_k) [11]:

$$\mathbf{u_s} = r_s \mathbf{i_s} + T_N \frac{d}{dt}\boldsymbol{\psi}_\mathbf{s} + j\omega_k \boldsymbol{\psi}_\mathbf{s} \tag{1}$$

$$\mathbf{0} = r_r \mathbf{i_r} + T_N \frac{d}{dt}\boldsymbol{\psi}_\mathbf{r} + j(\omega_k - \omega_1)\boldsymbol{\psi}_\mathbf{r} \tag{2}$$

$$\boldsymbol{\psi}_\mathbf{s} = x_s \mathbf{i_s} + x_M \mathbf{i_r} \tag{3}$$

$$\boldsymbol{\psi}_\mathbf{r} = x_r \mathbf{i_r} + x_M \mathbf{i_s} \tag{4}$$

$$m_e = \mathrm{Im}\left(\boldsymbol{\psi}_\mathbf{s}^* \mathbf{i_s}\right) \tag{5}$$

where: $\mathbf{u_s} = u_{s\alpha} + ju_{s\beta}$, $\mathbf{i_s}=i_{s\alpha} + ji_{s\beta}$, $\boldsymbol{\psi}_\mathbf{s} = \psi_{s\alpha}+j\psi_{s\alpha}$ – space vectors of the stator voltage, current and flux, $\mathbf{i_r} = i_{r\alpha} + ji_{r\beta}$, $\boldsymbol{\psi}_\mathbf{r} = \psi_{r\alpha}+j\psi_{r\beta}$ – space vectors of the rotor current and flux, r_s, x_s, r_r, x_r, x_M, – induction motor parameters: stator and rotor winding resistances, reactances and magnetizing reactance, ω_1 – motor speed, m_e – electromagnetic torque, $f_{sN} = 50$ Hz. Time constant $T_N = 1/(2\pi f_{sN})$ is a result of per unit system introducing, the base values can be found in [11].

3. Direct Torque Control with Space Vector Modulation

Direct Torque Control with Space Vector Modulation DTC-SVM, used for the induction motor drive control, can be classified to the constant flux control methods [10]. In this case stator flux amplitude is stabilized. It can be estimated from:

$$\hat{\boldsymbol{\psi}}_\mathbf{s} = x_M / x_r \hat{\boldsymbol{\psi}}_\mathbf{r} + x_s \sigma \mathbf{i_s} \tag{6}$$

where: the dash sign ^ – estimated value, $\sigma = 1-x_M^2/(x_s x_r)$.

Motor torque can be estimated using the following formula, defined in the stationary reference frame:

$$\hat{m}_e = \hat{\psi}_{s\beta} i_{s\alpha} - \hat{\psi}_{s\alpha} i_{s\beta} \tag{7}$$

Rotor flux can be estimated using one of the different estimators [12], [13].

The principle of the operation of the described control method is based on the analysis of the induction motor equations written in the coordinate system rotating with the stator flux vector velocity ($\omega_k=\omega_{\psi s}$, $\psi_{sx}=\psi_s$, $\psi_{sy}=0$), i.e.

$$u_{sx} = r_s i_{sx} + T_N \frac{d\psi_s}{dt} \tag{8}$$

$$u_{sy} = r_s i_{sy} + \omega_{\psi s}\psi_s \tag{9}$$

Torque equation (5) in this coordinate system, with $\omega_{\psi s}\psi_s$ decoupled:

$$m_e = \psi_{sx} i_{sy} - \psi_{sy} i_{sx} \xrightarrow[\omega_{\psi s}\psi_s \text{ decoupled}]{\psi_{sx}=\psi_s,\,\psi_{sy}=0} m_e = \frac{1}{r_s}\psi_s u_{sy} \tag{10}$$

A possibility of the stator flux amplitude control using the u_{sx} component results from equation (8). There appears a factor $\omega_{s\psi}\psi_s$ in (9) which decoupling allows (with constant ψ_s) to control the motor torque (10) using the u_{sy} component.

The simplest field-weakening is applied for the operation with motor speeds greater than the nominal value:

$$\psi_s^{ref} = \psi_{sN}\omega_{1N}/|\omega_1| \tag{11}$$

where: superscript *ref* – reference value, *N* – denotes the nominal value.

4. Two-mass drive system

Many industrial drive systems can be modelled as two-mass systems, where the first mass represents the moment of inertia of the motor and the second mass refers to the moment of inertia of the load machine. In this paper, the commonly used inertia-free-shaft dual-mass system model will be employed, which is described by the following normalized differential equations [14]:

$$T_1 \frac{d\omega_1(t)}{dt} = m_e(t) - m_s(t) \tag{12}$$

$$T_2 \frac{d\omega_2(t)}{dt} = m_s(t) - m_L(t) \tag{13}$$

$$T_c \frac{dm_s(t)}{dt} = \omega_1(t) - \omega_2(t) \tag{14}$$

$$T_x \frac{d\alpha(t)}{dt} = \omega_2(t) \tag{15}$$

where: ω_2 – load speed, m_s, m_L – shaft ad load torques, α – shaft position, T_1, T_2– mechanical time constant of the motor and the load machine, T_c – stiffness time constant and T_x – position time constant.

The schematic diagram of a dual-mass system is shown in Fig. 1.

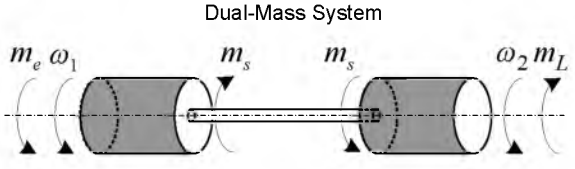

Fig. 1. The ideal diagram of the two-mass system

In most cases, the internal damping coefficient d is very small and can be neglected in the synthesis of the control system.

The resonant f_r and antiresonant f_{ar} frequencies of the two-mass system are defined as follows:

$$f_r = \frac{1}{2\pi}\sqrt{K_c \frac{J_1 + J_2}{J_1 J_2}}, \quad f_{ar} = \frac{1}{2\pi}\sqrt{\frac{K_c}{J_2}} \tag{16}$$

The value of the resonant frequency depends on the type of the drive and can vary from a few hertz in a paper machine section [15], through dozens of hertz in a rolling-mill drive [16], and can exceed hundreds hertz in a modern servo-drives [9]. The value of the antiresonant frequency can be even ten times smaller than the resonant one in a dryer [14], but usually the difference is much smaller (smaller than two).

Another parameter commonly provided for analysis of the two-mass system is the inertia ratio defined as:

$$R = \frac{J_2}{J_1} = \frac{T_2}{T_1} \tag{17}$$

The mechanical parameters of the drive are collected in Table 1.

Table 1. Mechanical parameters

T_1 [s]	T_2 [s]	T_c [s]	T_x [s]		f_r [Hz]	f_{ar} [Hz]	R [-]
0.02	0.05	0.001	0.5	1.5	22.5	42.1	2.5

5. MPC-based control structure

In model predictive control, an explicit model of the plant is used to predict the effect of future actions of the manipulated variables on the process output. The performance of the system (whether predicted or actual) will be assessed through a cost function [17, 18]:

$$J = \sum_{k=0}^{\infty} \mathbf{y}_{\mathbf{k}}^{\mathrm{T}} \mathbf{Q} \mathbf{y}_{\mathbf{k}} + \mathbf{u}_{\mathbf{k}}^{\mathrm{T}} \mathbf{R} \mathbf{u}_{\mathbf{k}} \tag{18}$$

where: $\mathbf{Q} \geq \mathbf{0}$ and $\mathbf{R} > \mathbf{0}$ are the weighting matrices.

In (18), $\mathbf{y_k}$ denotes the value of the output vector at a future time k, given an input sequence $\mathbf{u_k}$, an initial state $\mathbf{x_0}$ of the system. At each time step k an MPC algorithm attempts to optimize future plant behaviour while respecting the system input/output constraints by computing a sequence of control actions.

The MPC algorithm based on problem (18) can be implemented in two ways. The traditional approach relies on solving the optimization problem on-line for a given $\mathbf{x_k}$ in a receding-horizon fashion. This means that, at the current time k, only the first element control signal $\mathbf{u_k}$ of the optimal input sequence is actually implemented to the plant and the rest of the control moves $\mathbf{u_{k+I}}$ are discarded. At the next time step, the whole procedure is repeated for the new measured or estimated state $\mathbf{x_{k+1}}$ [18]. This strategy can be computationally demanding for systems requiring fast sampling or low-performance computers and hence greatly restricting the scope of applicability to systems with relatively slow dynamics. In the second approach, the problem (18) is first solved off-line for all state realizations $\mathbf{x} \in X_f$ with the use of multi-parametric programming [18]. Specifically, by treating the state vector x_k as a parameter vector, it can be shown that the parameter space X_f can be subdivided into characteristic regions, where the optimizer is given as an explicit function of the parameters. This profile is a piecewise affine state feedback law:

$$U(x) = K_r \mathbf{x} + \mathbf{g}_r, \qquad \forall x \in P_r \tag{19}$$

where P_r are polyhedral sets defined as:

$$P_r = \left\{ x \in \Re^n \mid H_r x \leq d_r \right\}, \qquad r = 1,\ldots N_r \tag{20}$$

Algorithms for the construction of a polyhedral partition of the state space and computation of a PWA control law are given in [18]-[23]. In its simplest form, the PWA control law (19)–(20) can be evaluated by searching for a region containing current state x in its interior and applying the affine control law associated with this region. More efficient search strategies which offer a logarithmic-type complexity with respect to the total number of regions Nr in the partition have also been developed. Nonetheless, the implementation of the explicit MPC control law can often be several orders of magnitude more efficient than solving the optimization problem (18) directly. This gain in efficiency is crucial for demanding applications with fast dynamics or high sampling rates in the mili/micro second range, such as the drive system considered in this paper. A more exact description of the MPC strategy and its explicit solution is presented in [18-23].

The disadvantage of the second solution is the lack of possibilities for adapting the parameters and constraints.

The block diagram of the considered control structure presented in Fig. 2.

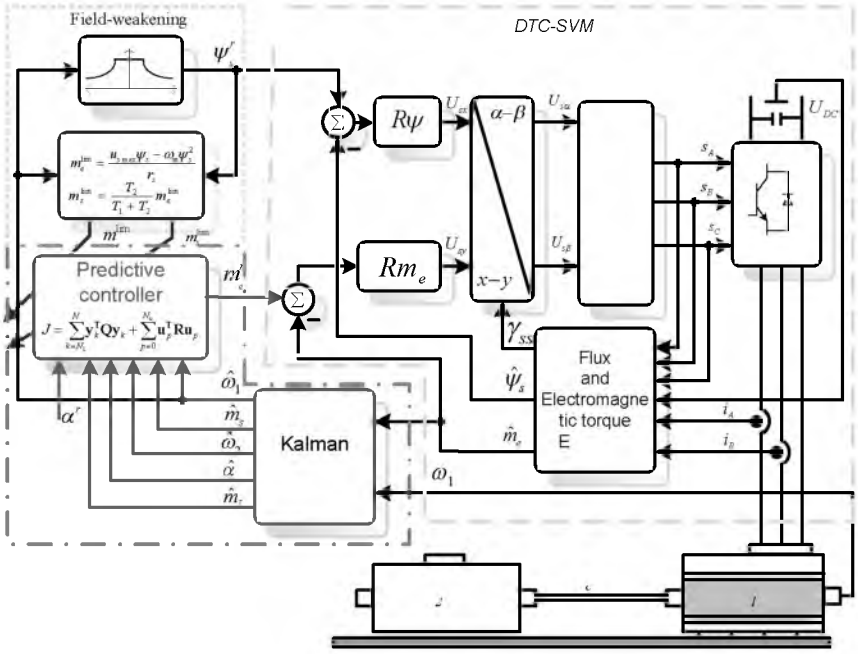

Fig. 2. The block diagram of the analysed control structure with MPC position controller

It consists of the following blocks:

- a dual-mass system,
- a DTC-SVM torque control loop,
- a predictive position controller,
- an electromagnetic torque adaptation block,
- a Kalman Filter used for estimation of the system state variables (it is assumed that only the motor speed are available for control purposes) [14].

The original state vector of the two-mass drive system has been extended by two additional variables which describe the dynamic of the load torque and reference shaft position value. The dynamics of the two mentioned variables is unknown so it is assumed:

$$\frac{d}{dt} m_L = 0 \tag{21}$$

$$\frac{d}{dt} \alpha^{ref} = 0 \tag{22}$$

Taking into account the abovementioned variables, the analysed state vector has the following form:

$$X_c = \left[\omega_1 \quad \omega_2 \quad m_s \quad \alpha \quad m_L \quad \alpha^{ref}\right]^T \tag{23}$$

The model described by eq. (11)-(14),(21)-(22) has been transformed to a discrete model with sampling time T_s. The following constraints are imposed for all k:

$$\begin{aligned} -2 \le m_e \le 2 \\ -1.2 \le m_s \le 1.2 \\ -1.2 \le \omega_2 \le 1.2 \end{aligned} \tag{24}$$

The vector $\mathbf{y_k}$ used in (18) has the following form:

$$\begin{aligned} y_1 &= \alpha - \alpha^{ref} \\ y_2 &= m_s - m_L \\ y_3 &= \omega^{ref} - \omega_1 \\ y_4 &= \omega^{ref} - \omega_2 \end{aligned} \tag{25}$$

The first term of (25) minimizes the difference between the load position and the reference value while the second term minimizes the difference between the shaft and the load torque and last terms calculate the differences between the two speeds and reference values. In this case the reference speed is chosen on the level zero.

The resulting formulation of (18) can be given in the following form:

$$\min_{u_1,u_2,\cdots,u_{Nc}-1} \sum_{k=0}^{N} q_1\left(y_1(k)\right)^2 + q_2\left(y_2(k)\right)^2 + q_3\left(y_3(k)\right)^2 + q_4\left(y_4(k)\right)^2 + \sum_{j=1}^{Nc-1} r\left(m_e^r(j)\right)^2 \tag{26}$$

where: $q_1 \ldots q_4$ – weights for the vector $\mathbf{y_k}$, r – weight for control signal, N – length of the horizon window, N_c – control horizon,

On the basis of the [24] a simple algorithm of changing the limit of the electromagnetic torque used during the optimization of the predictive controller can be introduced. The algorithm takes into consideration current and voltage constraints. The accurate derivation of the following condition can be found in the source article [24]:

$$m_e^{\lim} = \frac{u_{s\max}\psi_s - \omega_1\psi_s^2}{r_s} \tag{27}$$

where: $u_{s\max}$ – maximum available stator voltage value, ψ_s – amplitude of the stator flux.

The predictive regulator in order not to lose the ability to suppress the torsional vibrations during the operation with the constraints, the limit value of the torsional torque must be tuned with the limitation of the electromagnetic torque (27):

$$m_s^{\lim} = \frac{T_2}{T_1 + T_2} m_e^{\lim} \tag{28}$$

where: m_e^{lim} – actual limit value of the electromagnetic torque.

6. Results

In order to illustrate the operation and advantages of the presented predictive regulator the simulation tests were conducted. Influence of the reference position value and the position time constant on the ability of the operation in the field-weakening region were analysed. Parameters of the chosen regulator are gathered in Table 2.

Table 2. Parameters of the proposed regulator

N	N_c	$m_e^{max}e$	ω^{max}	q_1	q_2	q_3	q_4	r	T_s
44	4	0.9	1	420	15	5	5	1	2.5 ms

Electromechanical system is calculated in 5 μs steps. The Kalman Filter and the torque and flux regulators are calculated every 500 μs. The Space Vector Modulation operates with the 10 kHz frequency.

First, the shaft positioning for low reference values and larger positioning constant (T_x = 1.5) was examined. After the stabilization of the amplitude of the stator flux, the reference position step change to 0.1 occurred. After 0.5 s the nominal load torque was applied.

The obtained results are presented in Fig. 3. It can be seen from the presented transients, that the position follows the reference value very quickly, without any overregulation and with smooth braking. For this value of the reference position, the speed does not reach the limit value. In the presented figure a proper electromagnetic and torsional torques adaptation can be noticed. The critical torque value is not exceeded, what can be seen in [25].

Next, the influence of the greater speed limit value on the shaft positioning duration time was analysed for the positioning constant T_x=1.5. The higher value of the limit results in the field-weakening operation. In Fig. 4 a comparison of two situations is presented: first, the limit value of the speed is set on the nominal value, and second when the constraint is increased to the value of 1.4. It can be seen that the positioning time is shortened, and no overregulation preserved as well. In both cases the adaptation of the torsional and electromagnetic torque limits is applied.

Additionally, the drive behaviour with increased limits is examined for a system with low positioning constant (T_x = 0.5). In this case a noticeable overregulation can be seen when the speed limit is set on 1.4 (Fig. 5d). Q matrix values have almost no influence on the overregulation (it is possible to reduce it, but it implies a multiple prolonging of the positioning time, what is not acceptable).

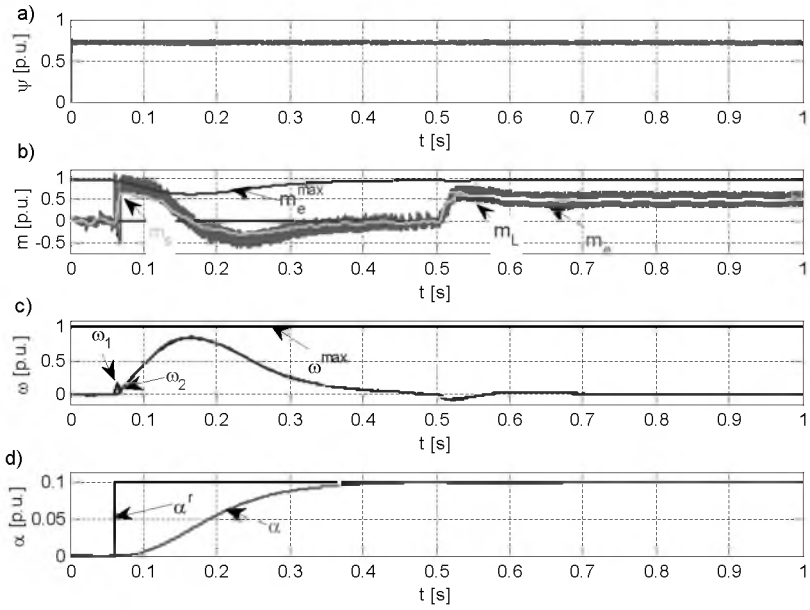

Fig. 3. Control structure operation for larger position time constant and low reference value: a) stator flux amplitude, b) torque, c) speed, d) reference and actual shaft position

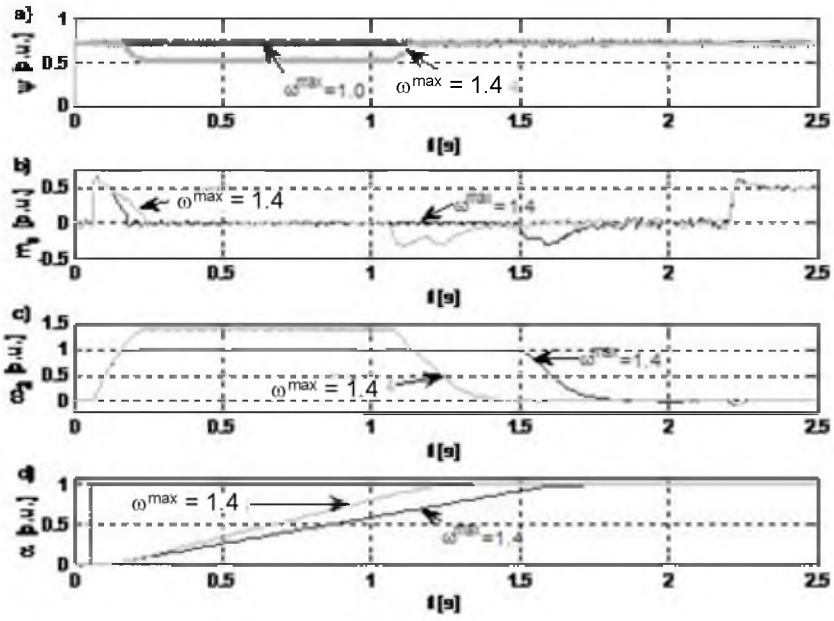

Fig. 4. Control structure performance for two different speed limits for larger position time constant: a) stator flux amplitude, b) torsional torque, c) load speed, d) shaft position

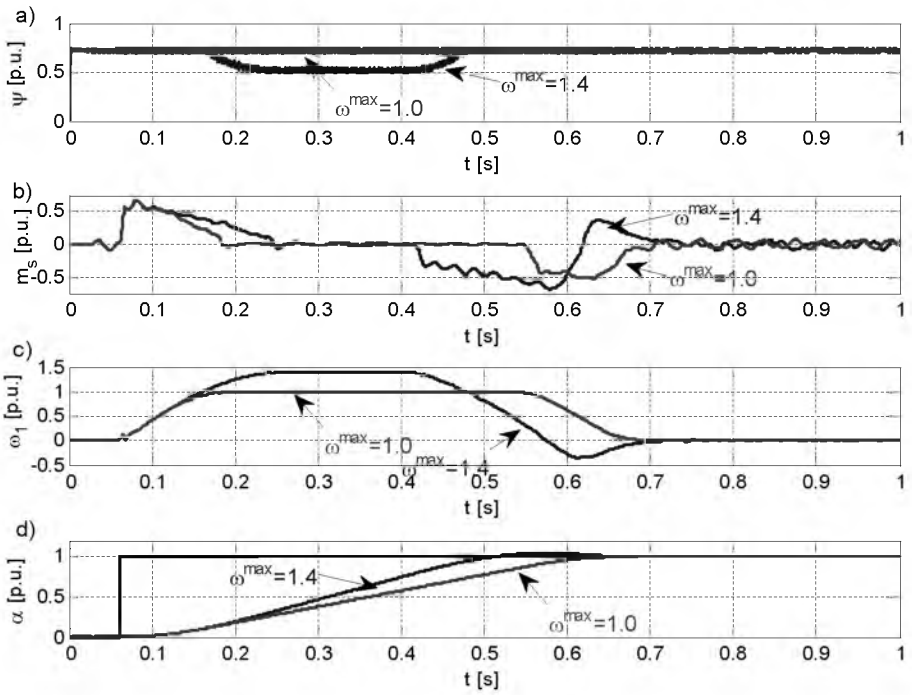

Fig. 5. Smaller position time constant – comparison of two values of the speed limit: a) stator flux amplitude, b) torque, c) speed, d) shaft position

7. Summary

A concept of a predictive position controller co-operating with the Direct Torque Control – Space Vector Modulation for the two-mass induction motor drive is presented in the paper. The control structure is extended with the mechanism of the electromagnetic and torsional torque limits adaptation. Applying this mechanism allows to eliminate the possibility of exceeding the critical torque.

Increasing the speed limit over the nominal value, i.e. the field-weakening operation allows to shorten the time of the shaft positioning. However, an undesirable overregulation appears when the time constants in the system are small. For this reason an application of an additional decision block will be necessary, which will select the speed limit on the basis of the reference position value.

Within the framework of the future works a practical verification of the obtained results on a laboratory setup is planned, as well as the development of the speed limit adaptation algorithm.

Work funded by the National Science Centre within the agreement: UMO-2011/01/N/ST7/04544 (2011-2013)

References

[1] Deur J., Peric N., *Pointing and tracking position control system of electrical drives with elastic transmission*, 9th Int. Conf. and Exhibition on Power Electronics and Motion Control - EPE PEMC, Kosice, Slovak Republic, 2000.

[2] Schutte E., Beineke S., Rolfsmeier A., Grotstollen H., *Online Identification of Mechanical Parameters Using Extended Kalman Filters*, Ind. Appl. Conf. IAS'97, New Orleans, 1997.

[3] Seiji Hashimoto, Kenji Hara, Hirohito Funato, Kenzo Kamiyama, *AR-Based Identification and Control Approach in Vibration Suppression*, IEEE Trans. on Ind. Appl., vol. 37, no. 3, pp. 806-811, 2001.

[4] Dodds S.J., Perryman R., Rapsik M., Vittek J., *Forced dynamics control of electric drives employing PMSM with a flexible coupling*, Australasian Universities Power Engineering Conf.,. AUPEC, 2007.

[5] Vittek J., Makys P., Stulrajter M., Dodds S.J., Perryman R., *Comparison of sliding mode and forced dynamics control of electric drive with a flexible coupling employing PMSM*, Int. Conf. on Industrial Technology, ICIT, 2008.

[6] Serkies P. *Comparison of dynamic properties of position control structures in two-mass drive with the classic cascade and FDC controller.,* Scientific Papers of Institute of Electrical Machines Drives and Measurements no. 65 Studies and Research no. 31, pp. 330-334, 2011 (in Polisch).

[7] Fitri M, Yakub M., Martono W., Akmeliawati R., *Vibration Control of Two-Mass Rotary System Using Improved NCTF Controller for Positioning Systems*, Control and System Graduate Research Colloquium, ICSGRC, 2010.

[8] Serkies P., Szabat K., *Predictive position control of the drive system with elastic joint*, Electrical Review vol. 87, no. 7, 276-279, 2011 (in Polish).

[9] Serkies P., Szabat K., *Application of the MPC controller to the Position Control of the Two-Mass Drive System*, IEEE Trans. on Industrial Electronics, Issue: 99, 2012 Early Access Articles.

[10] Buja G. S., Kaźmierkowski M. P., *Direct torque control of PWM inverter-fed AC motors - a survey*, IEEE Trans. on Ind. Electronics, vol. 51, no.4, pp.744-757, 2004.

[11] Orłowska-Kowalska T., *Speed sensorless induction motor drives*, Wrocław University of Technology Press, 2003 (in Polish).

[12] Orłowska-Kowalska T., Dybkowski M., Tarchała G., *Analysis of chosen speed estimators in induction motor drives – part I – mathematical models*, Scientific Papers of the Institute of Electrical Machines, Drives and Measurements of Wroclaw Univ. of Technology, no. 64, ser. Studies and Materials, no. 30, pp. 151-161, 2010 (in Polish).

[13] Dybkowski M., Orłowska-Kowalska T., Tarchała G., *Analysis of chosen speed estimators in induction motor drives – part II – test results*, Scientific Papers of the Institute of Electrical Machines, Drives and Measurements of Wroclaw Univ. of Technology, no. 64, ser. Studies and Materials, no. 30, pp. 162-175, 2010 (in Polish).

[14] Szabat K. *Control structures for electrical drive systems with elastic joints,* Scientific Papers of Institute of Electrical Machines Drives and Measurements no. 61, Monographs no. 19 (in Polish).

[15] Valenzuela M. A., Bentley J. M. and Lorenz R. D., *Evaluation of Torsional Oscillations in Paper Machine Sections*, IEEE Trans. on Ind. Appl., vol. 41, no. 2 , pp. 493-501, 2005.

[16] Wang J., Zhang Y., Xu L., Jing Y. and Zhang S. *Torsional vibration suppression of rolling mill with constrained model predictive control*, 6th World Congress on Intelligent Control and Automation, 2006, pp. 6401-6405, China.

[17] P. Taewski, *Advanced industrial control algorithms and structures*, EXIT 2002 (in Polish).

[18] Maciejowski J.M., *Predictive Control with Constraints*, Prentice Hall, UK, 2002.

[19] Cychowski M. T., *Robust Model Predictive Control*, VDM Verlag, 2009.

[20] Kvasnica M., Grieder P., Baotic M., and Morari M., *Multi-Parametric Toolbox (MPT), HSCC (Hybrid Systems: Computation and Control),* Lecture Notes in Computer Science, vol. 2993, 2004, pp. 448-460.

[21] Tøndel P., Johansen T.A. and Bemporad A. *An algorithm for multi-parametric quadratic programming and explicit MPC solutions*, Automatica, vol. 39, n0. 3. pp. 489-497, 2003.

[22] Spjøtvold J., Kerrigan E.C., Jones C.N., Tøndel, P., and Johansen T.A.*: On the facet-to-facet property of solutions to convex parametric quadratic programs*, Automatica, vol. 42, no. 12, pp. 2209-2214, 2006.

[23] Bemporad A., Morari M., Dua V., Pistikopoulos E. N., *The explicit linear quadratic regulator for constrained systems*, Automatica, vol. 38, no. 1, pp. 3-20, 2002.

[24] Wójcik P. Kaźmierkowski M.P., *Torque and flux control of induction machine drive in flux weakening region*, Scientific Papers of Institute of Electrical Engineering, vol. 239, pp. 131-142, 2008 (in Polish).

[25] Serkies P., *Predictive speed control in induction two-mass drive*. Poznan University of Technology Academic Journals. Electrical Engineering, vol. 72, pp. 149-156, 2012 (in Polish).